

# CHEMISTRY

## A European Journal

A Journal of



### Accepted Article

**Title:** Structure Enabled Discovery of a Stapled Peptide Inhibitor to Target the Oncogenic Transcriptional Repressor TLE1

**Authors:** Sally McGrath, Marcello Tortorici, Ludovic Drouin, Savade Solanki, Lewis Vidler, Isaac Westwood, Peter Gimeson, Rob vanMontfort, and Swen Hoelder

This manuscript has been accepted after peer review and appears as an Accepted Article online prior to editing, proofing, and formal publication of the final Version of Record (VoR). This work is currently citable by using the Digital Object Identifier (DOI) given below. The VoR will be published online in Early View as soon as possible and may be different to this Accepted Article as a result of editing. Readers should obtain the VoR from the journal website shown below when it is published to ensure accuracy of information. The authors are responsible for the content of this Accepted Article.

**To be cited as:** *Chem. Eur. J.* 10.1002/chem.201700747

**Link to VoR:** <http://dx.doi.org/10.1002/chem.201700747>

Supported by  
**ACES**

WILEY-VCH

# Structure Enabled Discovery of a Stapled Peptide Inhibitor to Target the Oncogenic Transcriptional Repressor TLE1.

Sally McGrath,<sup>[a]</sup> Marcello Tortorici,<sup>[a]</sup> Ludovic Drouin,<sup>[a]</sup> Savade Solanki,<sup>[a]</sup> Lewis Vidler,<sup>[a]</sup> Isaac Westwood,<sup>[a]</sup> Peter Gimeson,<sup>[b]</sup> Rob Van Montfort,<sup>[a]</sup> Swen Hoelder\*<sup>[a]</sup>

**Abstract:** TLE1 is an oncogenic transcriptional co-repressor that exerts its repressive effects through binding of transcription factors. Inhibition of this protein-protein interaction represents a putative cancer target but no small molecule inhibitors have been published for this challenging interface. In this manuscript, we report the structure enabled design and synthesis of a constrained peptide inhibitor of TLE1. Our design featured introduction of a four carbon atom linker into the peptide epitope found in many TLE1 binding partners. We developed a concise synthetic route to a proof of concept peptide cycFWRPW. Biophysical testing by ITC and thermal shift assays showed that whilst the constrained peptide bound potently, it had an approximately five fold higher  $K_d$  than the unconstrained peptide. Our co-crystal structure suggested that the reduced affinity is likely due to a small shift of one side-chain compared to the otherwise well conserved conformation of the acyclic peptide. Our work describes a constrained peptide inhibitor that may serve as the basis for improved inhibitors.

## Introduction

TLE proteins (Transducin-Like Enhancer proteins) are transcriptional co-repressors that modulate key pathways for developmental as well as oncogenic signalling such as the Notch and Wnt pathway. The TLE proteins do not bind directly to DNA to exert their repressive effect on gene transcription. Instead they utilise their WDR domains to bind to DNA bound transcription factors.<sup>[1]</sup> Given their role in pathways known to be deregulated in many cancers, it is not surprising that members of the TLE family, particularly TLE1 have been implicated in the development and maintenance of malignancies. Elevated levels of TLE1 have been observed in a growing list of tumours, including cervical, lung and colon carcinomas and TLE1 has been recognised as a putative oncogene.<sup>[2]</sup> Given that TLE1 does not bind to DNA directly and that its repressive and potentially oncogenic role relies on the ability of the WDR domain to bind to transcription factors, blocking of this interaction has been suggested as a possible treatment for

cancers with elevated TLE1 activity.<sup>[3]</sup> However, to date no TLE inhibitors have been described in the literature.

The crystal structures of the WDR domain of TLE1 in complex with peptides derived from two different transcription factor binding partners have been solved, thus characterising the binding interface in detail.<sup>[3]</sup> One of these peptides (SMWRPW) shows relatively potent ( $K_d = 1 \mu\text{M}$ ) binding to TLE1. As will be discussed in more detail below, the bioactive conformation of this peptide is characterised by a compactly folded core formed by the central three amino acids. This compact core engages in extensive interactions with the WDR1 domain and positions key amino acid side-chains such that they can form additional polar and non-polar interactions (vide infra).<sup>[3]</sup> Given that this peptide binds with micromolar activity and that detailed knowledge of its binding mode and bioactive conformation are available, it represents an attractive starting point for the discovery of TLE inhibitors. Here we report a peptidomimetic approach based on the hypothesis that the compact conformation of this peptide can be stabilised by a hydrocarbon linker.

Hydrocarbon stapled macrocyclic peptides are increasingly being explored as drug candidates and chemical probes, particularly for challenging targets such as protein-protein interactions.<sup>[4]</sup> Introducing conformational constraint through macrocyclisation has a number of benefits. It particularly reduces the entropic penalty upon binding to the target and has been shown to have the potential to improve cell penetration and metabolic stability.<sup>[5]</sup>

[a] Dr. S. McGrath, Dr. M. Tortorici, Dr. L. Drouin, Dr. S. Solanki, Dr. L. Vidler, Dr. I. Westwood, Dr. R. Van Montfort, Dr. S. Hoelder  
The Institute of Cancer Research  
Division of Cancer Therapeutics Unit  
Cancer Research UK Cancer Therapeutics Unit  
15 Costwold Road, Sutton, Surrey, SM2 5NG, UK  
Phone: +44 2087224353  
E-mail: swen.hoelder@icr.ac.uk

[b] P. Gimeson  
Malvern Instruments Nordic AB  
Vallongatan 1, Uppsala, 752 28, Sweden  
Phone: +46 704411919  
E-mail: peter.gimeson@malvern.com

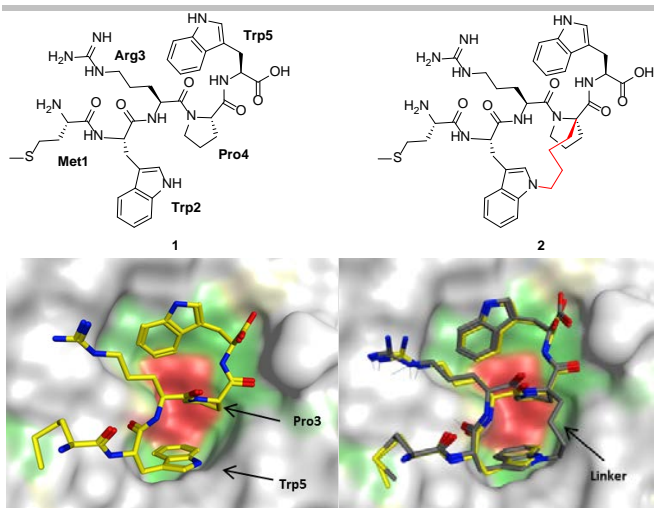


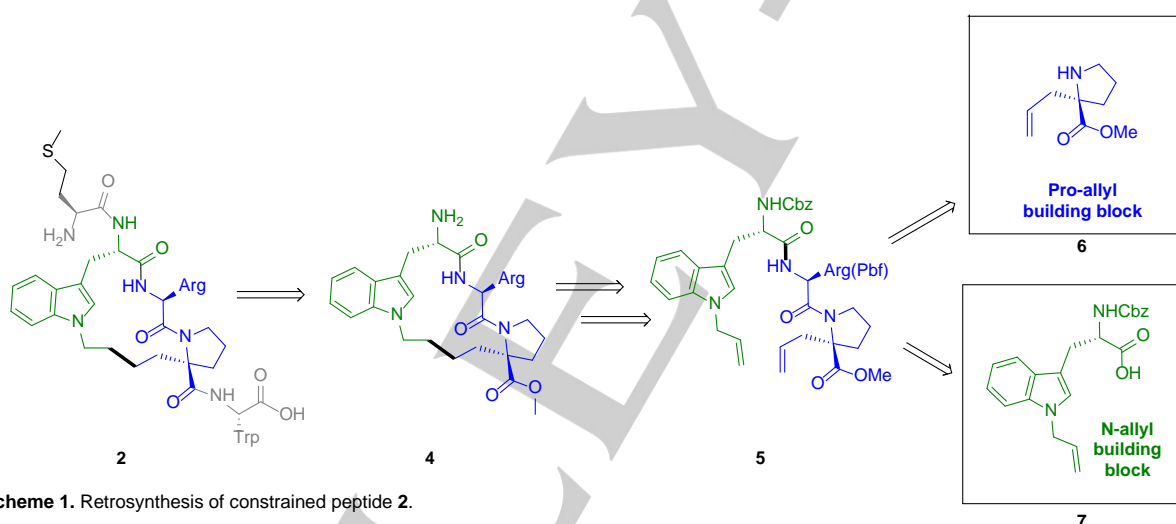
**Figure 1:** Upper panel. Chemical structures of the SMWRPW peptide **1** and the constrained peptide **2** (the linker is drawn in red) Lower panel. Co-crystal structure of SMWRPW bound to the WDR domain of TLE1 (pdb code 2CE9) and superposition of the modelled binding pose of the constrained peptide with the crystallised pose of the unconstrained peptide **1**.

the structure of the constrained peptide bound to the WDR domain of TLE1.

### Design

The crystal structure of the SMWRPW peptide bound to the WDR domain of TLE1 was obtained by soaking apo TLE1 crystals in a solution of the slightly extended SMWRPW peptide.<sup>[3]</sup> The indole moiety of the N-terminal tryptophan (Trp5) and the central proline (Pro3) of the bound peptide tightly pack against each other forming the core of the binding epitope (Figure 1). This core engages in extensive hydrophobic interaction with the protein.

The compact conformation positions sidechains and backbone moieties of the peptide such that they are ideally placed to engage in additional polar and hydrophobic interactions.<sup>[3]</sup> The N-terminal serine residue of the SMWRPW peptide is not resolved, suggesting that it is disordered and does not make any specific interactions.



**Scheme 1.** Retrosynthesis of constrained peptide **2**.

Designing and synthesising constrained macrocyclic peptides still remains a formidable challenge.<sup>[4]</sup> Nevertheless, successful examples have been reported, particularly for constraining and stabilising  $\alpha$ -helices,  $\beta$ -sheets and  $\beta$ -turns.<sup>[4]</sup>

However, in the case of TLE1, the bound SMWRPW peptide adopts neither a typical  $\alpha$ -helical nor a  $\beta$ -sheet conformation and constraining the peptide thus required a different strategy. As will be described in more detail below, we hypothesised that connecting two amino acids that are a critical part of the binding epitope, the side-chain of the first tryptophan and the proline, through a hydrocarbon linker would stabilise the bioactive conformation. Here we report the design and development of a chemical route to this hydrocarbon linker-constrained, proof of concept peptide. Furthermore we tested the binding affinity of the constrained and corresponding acyclic peptides and solved

Our strategy to generate a constrained macrocyclic inhibitor is illustrated in figure 1: we hypothesised that connecting the C $\alpha$ -atom of the proline residue and the N1 nitrogen of the N-terminal tryptophan with a hydrocarbon linker will lock the peptide in the bioactive conformation. We modelled various linker lengths in MOE by introducing the linker in silico into the bound conformation of the peptide (PDB code 2CE9) and energy minimising the modified peptides in the TLE binding site. The resulting poses were visually inspected for minimal movement of the peptide sidechains and low energy conformations of the linker. These experiments together with an analysis of synthetic accessibility (see below) suggested an ideal length of 4 carbon atoms and compound **2** (Figure 1) as a promising synthesis target.

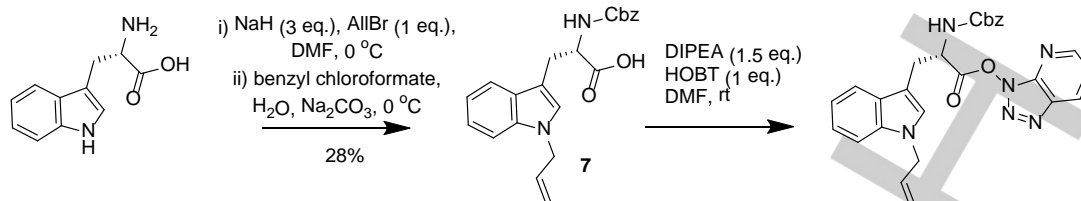
### Retrosynthesis

## FULL PAPER

WILEY-VCH

Our retrosynthetic analysis is depicted in Scheme 1. We envisioned synthesising the constrained hydrocarbon stapled

unprotected L-tryptophan using either a copper TMEDA catalyst or sodium metal had been described.<sup>[6]</sup> We tested the copper



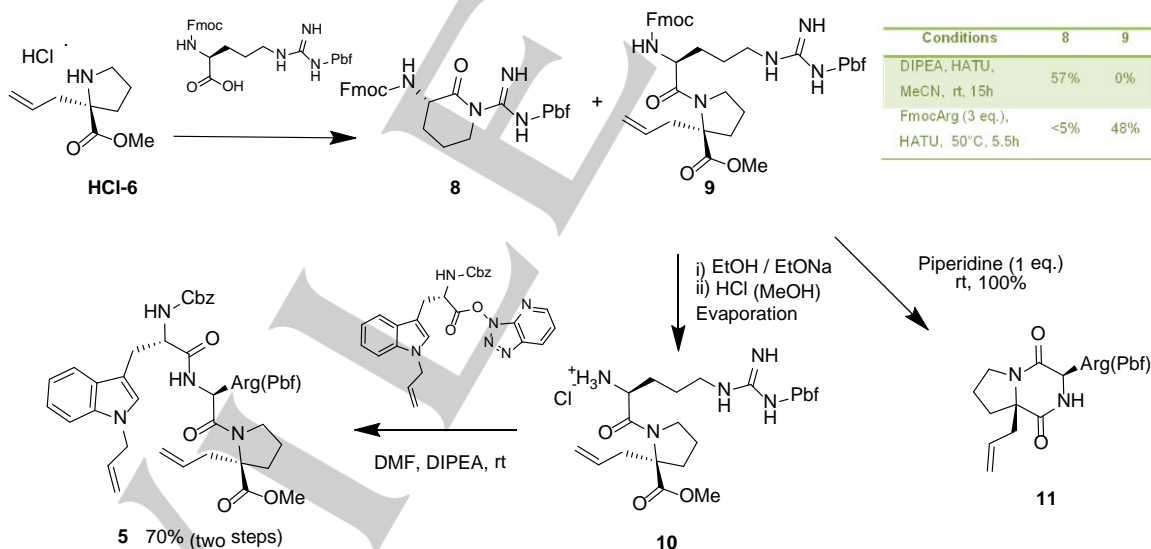
**Scheme 2.** Synthesis of N-allyl-Trp 7.

peptide **2** from the macrocyclic intermediate **4** through addition of the N-terminal methionine and the C-terminal tryptophan via peptide coupling chemistry. Furthermore, we hypothesised that intermediate **4** can be prepared from the acyclic tripeptide **5** through RCM, followed by concomitant saturation of the double bond and removal of the Cbz protecting group under hydrogenation conditions. To prepare the acyclic RCM precursor **5**, two unnatural amino acids were required, substituted proline **6** and allyl substituted tryptophan **7**.

This approach offered the advantage of conducting the critical RCM in solution whilst all polar groups, particularly the basic arginine side-chain were fully protected. Furthermore the cyclic intermediate **4** offered the opportunity of late stage modification of the C- and N-terminal amino acids.

## Results and discussion

mediated conditions but did not observe any conversion. More recently a team from Sanofi published the synthesis of boc protected 1-allyl-L-tryptophan but this work was not in the public domain when we undertook our work.<sup>[7]</sup> We hypothesised that selective allylation of unprotected tryptophan can be achieved after deprotonating the carboxyl group and the NH indole with two equivalents of a strong base such as NaH, since under these conditions the deprotonated indole nitrogen represents the strongest nucleophile. Pleasingly, reacting L-tryptophan with 2.5 equivalents of NaH and one equivalent of allyl bromide in DMF gave the desired mono allylated product in 40% yield after HPLC purification. To avoid HPLC purification of the polar, unprotected amino acid we decided to attempt the allylation and subsequent Cbz protection with benzyl chloroformate in a one pot procedure. Gratifyingly, this procedure gave the desired, protected amino



**Scheme 3.** Optimised reaction conditions for the synthesis of arginine containing tripeptide **5**.

The synthesis of the proline derivative **6** was described in the literature and we followed the protocols with minor modifications. We next turned our attention to the synthesis of Cbz protected 1-allyl-L-tryptophan **7**. We decided to use the Cbz protecting group since it is stable to basic and acidic conditions and because we anticipated that it can easily be removed during hydrogenation of the double bond arising from the RCM thus making an additional step unnecessary. At the start of this work direct allylation of

acid **7** in an acceptable yield of 28% over two steps.

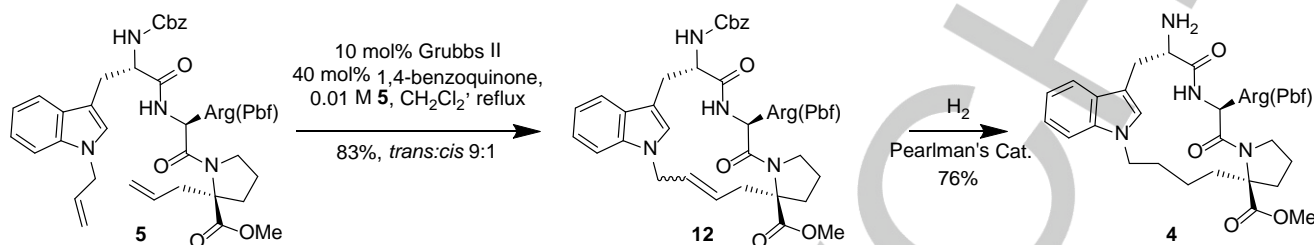
We next prepared the tripeptide RCM precursor **5** by coupling the allylated proline with protected arginine (Scheme 3) under conditions precedent for this proline derivative. However, we only isolated the cyclised side product **8**. The formation of this side product is likely due to steric hindrance of the amine functionality. Gratifyingly, increasing the reaction temperature

## FULL PAPER

WILEY-VCH

and the concentrations of the reactants to favour biomolecular reaction led to the desired dipeptide in 48% yield.

Next we attempted removal of the Fmoc protecting group from dipeptide **9** (Scheme 3). However, standard conditions using piperidine as the base gave the undesired side product **11** as a single diastereomer.



**Scheme 4:** Ring Closing Metathesis of **5**, removal of Cbz and double bond hydrogenation.

Repeating the reaction with 1 equivalent of piperidine and at a lower temperature (0 °C) resulted in a mixture of the unprotected dipeptide and the side product. Unfortunately, all attempts to isolate the unprotected dipeptide and to remove the piperidine, resulted in complete conversion to the diketopiperazine **11** side product. To solve this conundrum we reasoned that protonation after Fmoc deprotection will lower the nucleophilicity of the free amino group sufficiently to prevent cyclisation thus allowing isolation by evaporation of the solvent. Furthermore, we tested alternative bases, particularly bases likely to not affect the subsequent peptide coupling step. This approach indeed proved successful and compound **HCl-10** was obtained as single stereoisomer through clean Fmoc deprotection in EtOH using one equivalent of NaOEt as base. Subsequent protonation of the amine and residual traces of NaOEt by addition of an HCl solution in MeOH thwarted formation of the side product upon solvent evaporation (Scheme 3). Coupling of the crude product with the HATU derivative of the allyl substituted tryptophan **7** using DIPEA as a base yielded the metathesis precursor **5** in 70% overall yield.

To our delight, the pivotal RCM proceeded readily using Grubbs' second generation catalyst<sup>[8]</sup> in the presence of 1,4-benzoquinone<sup>[9]</sup> yielding the desired product **12** in 83% yield as a 9:1 mixture of *trans* and *cis* isomers (Scheme 4).

We next investigated concomitant reduction of the double bond and removal of the Cbz group by hydrogenation (Scheme 4). Commonly used conditions such as 10% palladium on carbon

and hydrogen at atmospheric pressure left the starting material intact. Elevated temperature, addition of acid or increase of catalyst loading did not significantly improve turnover. We next investigated other catalysts and found that Pearlman's catalyst both reduced the double bond and removed the Cbz protecting group. Complete conversion required one equivalent of

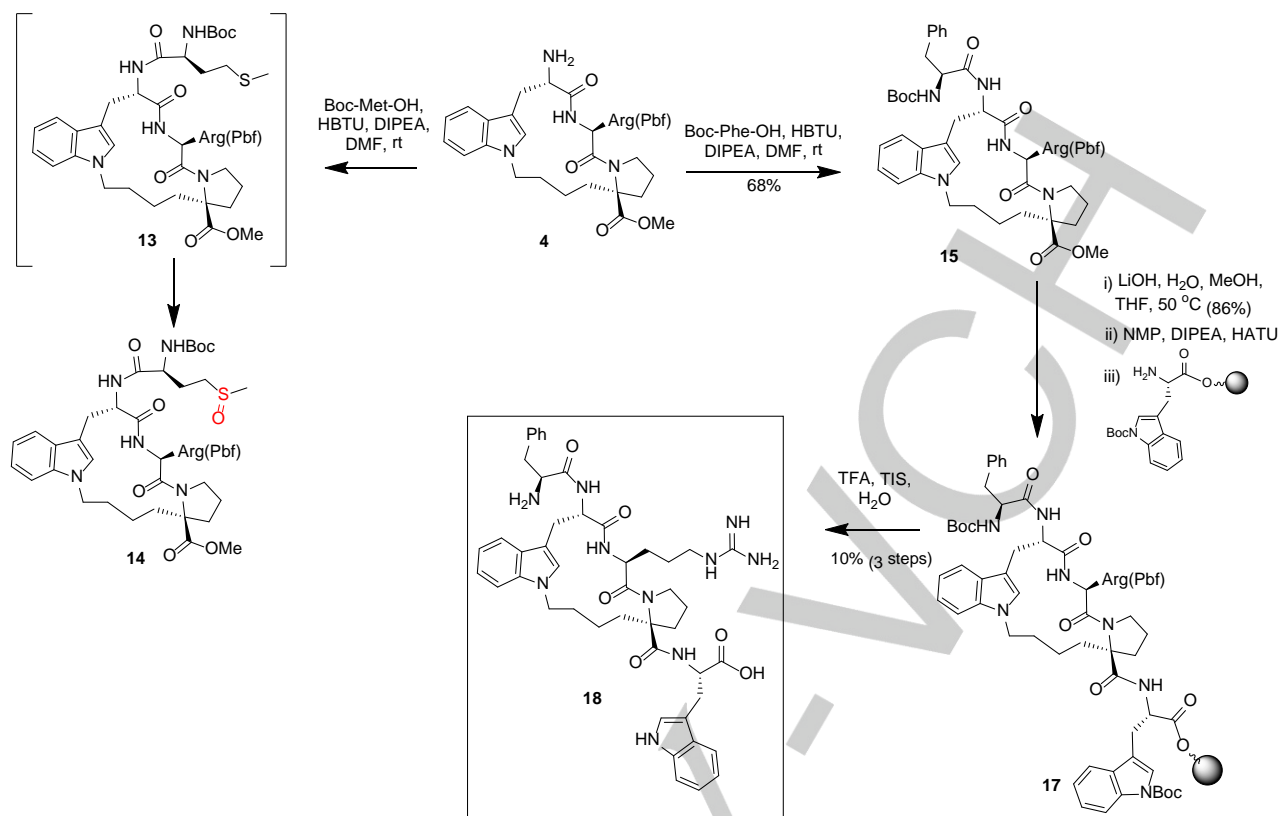
Pd(OH)<sub>2</sub>/C and the addition of 2 equivalents of HCl, but resulted in an isolated yield of 76% of the reduced and deprotected intermediate.

With intermediate **4** in hand we next performed the coupling to Boc-protected methionine. Whilst this coupling proceeded readily, we reproducibly observed a +16 Da increase in molecular weight after isolation and purification. We attributed this increase to oxidation of the methionine to the corresponding sulfoxide derivative **14** (Scheme 5). This oxidation is preceded in the literature, however the degree and rapidness of the reaction was surprising given that methionine is frequently incorporated into peptides.

As we will discuss in the more detail below, this methionine residue can be replaced in the acyclic peptide by phenylalanine without loss of activity. We thus focused our attention on the phenylalanine derivative. Coupling of **4** with Boc-protected phenylalanine proceeded in 68% yield after purification (Scheme 5).

To complete the synthesis we hydrolysed the ester using LiOH in methanol (86% yield) and added the final amino acid by coupling this intermediate onto commercially available solid support bound tryptophan (Scheme 5).

Cleavage of the solid support of **17** and concomitant removal of the remaining two protecting groups provided the desired macrocyclic peptide **18** in 10% yield over three steps (Scheme 5).



**Scheme 5.** Synthesis of the final constrained peptide **18**.

Despite initial challenges, our synthetic approach enabled us to access 14 mg of the desired, constrained peptide. Some of the optimised steps, e.g. the one pot alkylation and protection of tryptophan as well as the convenient and mild deprotection of the Fmoc group in solution may be useful for the synthesis of other constrained peptides.

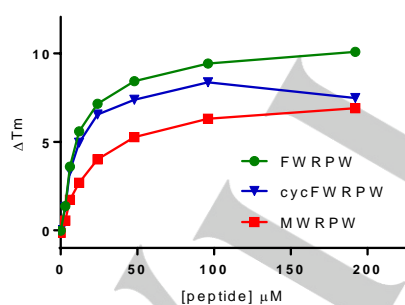


**Figure 2.**  $\Delta T_m$  plot of peptides-hTLE1 443-770 interaction in thermal shift experiments. All the measurements were carried out in triplicate and the points are reported as mean  $\pm$  SD. The  $\Delta T_m$  at top concentrations is also reported in the table.

We next investigated the binding of this macrocyclic as well as the acyclic MWRPW and FWRPW peptides to TLE1. We used two orthogonal binding assays, the thermal shift assay<sup>[10]</sup> and isothermal titration calorimetry (ITC)<sup>[11]</sup> to test binding of **18** and the linear peptides to the TLE1 WD40 domain (TLE1 residues 443-770). The thermal shift data for the three peptides are shown in figure 2 and table 1.

All three peptides showed significant thermal shifts indicative of binding to the protein. Interestingly, the MWRPW peptide, which is derived from the sequence of TLE1 binding partners shows

**Table 1.** Thermal shifts at 100 and 200  $\mu$ M peptide concentrations.

Peptide Ligand	$\Delta T_m$ (100 $\mu$ M)	$\Delta T_m$ (200 $\mu$ M)
MWRPW	6.3°C	6.9°C
cycFWRPW ( <b>18</b> )	8.4°C	7.5°C
FWRPW	9.4°C	10.1°C

the smallest thermal increase. The mutant FWRPW peptide causes a significantly larger thermal shift (9.4 °C versus 6.3 °C). The cyclic peptide cycFWRPW (**18**) at 100  $\mu$ M shows a thermal shift comparable to the corresponding acyclic peptide (Table 1). However, the thermal shift decreases when the concentration is further increased from 100 to 200  $\mu$ M. This decrease is likely due to precipitation of the peptide at higher concentrations. Our thermal shift data thus suggested that all three peptides bound to TLE1.

To confirm these findings and to explore the enthalpic and entropic contributions to binding of the linear and constrained

## FULL PAPER

WILEY-VCH

peptides we performed ITC experiments. Given conformational restriction, one might expect the constrained peptide to show a smaller entropic penalty upon binding. However, all three peptides showed potent binding driven by strong enthalpy contributions.

Interestingly, for each peptide we observed a biphasic curve. This was initially more pronounced for FWRPW and cycFWRPW (**18**) but also recognisable for the MWRPW peptide (see Supporting Information, Figure S1). We repeated the MWRPW titration at slightly higher protein and peptide concentrations to achieve a higher enthalpy signal and therefore better resolution of the titration event. Under these conditions we also observed a clear biphasic curve (Figure 4). The biphasic curves are indicative of two binding events and we calculated the thermodynamic data for both (Table 2).

The first phase of the curves corresponded to a molar ratio of

between the different peptides is in agreement with this hypothesis.

In the following paragraph we will focus the discussion of the ITC results on the second binding event ( $K_d2$ ,  $\Delta H2$  and  $-T\Delta S2$ ) for three reasons. The second binding event covers binding to the large majority of the protein (~80%), the  $K_d$ s are in agreement with published values and finally, due to the experimental set up, the relative errors are smaller. However, we include the data for the first binding event ( $K_d1$ ,  $\Delta H1$  and  $-T\Delta S1$ ) and they broadly follow the same trend.

The rank order based on the ITC  $K_d$ s ( $K_d2$ ) confirms the rank order from the thermal shift assay described above. The acyclic FWRPW shows the highest affinity with a  $K_d$  of 79 nM. It thus shows almost 10-fold more potent binding than the peptide representing the original MWRPW sequence from the TLE1 binding partners. The  $K_d2$  for the cyclic peptide **18** is 522 nM and

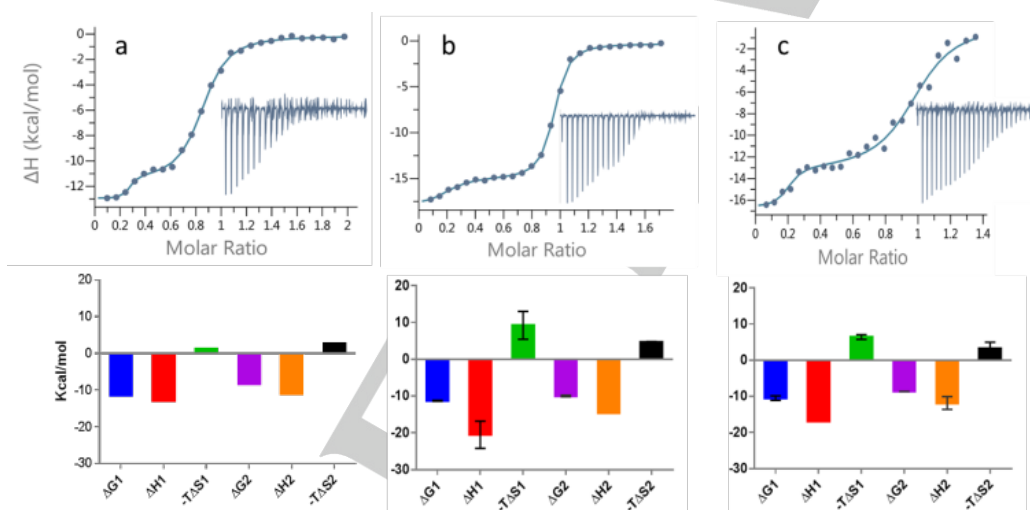


**Figure 4.** ITC measurement of peptides-TLE1 binding. Data fitting to a two-sites independent binding model, integrated heats are shown in the inset. Histograms showing  $\Delta G$ ,  $\Delta H$ , and  $-T\Delta S$  are presented in the bottom part of the figure. The thermodynamic values are also presented in Table 1. a. MWRPW-TLE1 binding,  $n=1$ . Experiment performed with TLE1 40  $\mu\text{M}$  and MWRPW peptide 420  $\mu\text{M}$ . b. FWRPW-TLE1 binding,  $n=2$ . Experiment performed with TLE1 30  $\mu\text{M}$ , FWRPW peptide 240  $\mu\text{M}$  and then repeated with TLE1 24  $\mu\text{M}$ , FWRPW peptide 180  $\mu\text{M}$ . Histograms represent averaged values, error bars denote SD. c. cyc-FWRPW-TLE1 binding,  $n=2$ . Experiment performed with TLE1 30  $\mu\text{M}$ , cyc-FWRPW 200  $\mu\text{M}$  and then repeated with TLE1 30  $\mu\text{M}$ , cyc-FWRPW 180  $\mu\text{M}$ . Histograms represent averaged values, error bars denote SD.

**Table 2.**  $K_d$  and thermodynamic values determined in ITC for all the peptides-TLE1 binding experiments.

	N1	$K_d1$ (nM)	$\Delta H1$ (kcal/mol)	$-T\Delta S1$ (kcal/mol)	N2	$K_d2$ (nM)	$\Delta H2$ (kcal/mol)	$-T\Delta S2$ (kcal/mol)
MWRPW	$0.24 \pm 0.001$	$3.5 \pm 1.9$	$-12.8 \pm 0.2$	1.3	$0.6 \pm 0.004$	$772 \pm 7.1$	$-11.1 \pm 0.11$	2.72
FWRPW	$0.18 \pm 0.002$	$8.6 \pm 3.9$	$-20.5 \pm 3.7$	$9.2 \pm 3.8$	$0.7 \pm 0.004$	$79.4 \pm 24.6$	$-14.6 \pm 0$	$4.6 \pm 0.2$
cyc-FWRPW	$0.18 \pm 0.01$	$24.7 \pm 24.2$	$-16.9 \pm 0$	$6.4 \pm 0.6$	$0.8 \pm 0.01$	$522 \pm 39.6$	$-11.8 \pm 1.8$	$3.2 \pm 1.7$

approximately 0.2 (that is 20% of the protein is bound) and the second an approximate molar ratio of 0.8 and the overall curve thus reached saturation at a molar ratio close to one. This suggested that only one binding site per molecule of protein is occupied by the ligand. A possible explanation for the biphasic curve is that in the binding experiment the protein exists in two conformations that do not rapidly interconvert and show different binding affinities for the peptides. The observation that the molar ratios for the two parts of the biphasic curve correspond

thus less potent than the corresponding acyclic peptide suggesting that introduction of the hydrocarbon linker leads to a small loss of activity. Interestingly, binding of **18** is accompanied by a reduced loss of entropy compared to the acyclic peptide which is in agreement with the hypothesis that introduction of a constraint reduces the entropic penalty (albeit that this reduced entropic loss is overcompensated by a larger enthalpic loss leading to a higher  $K_d$  compared to the acyclic FWRPW peptide).

To be able to interpret these thermodynamic data in light of the binding modes we set out to determine the crystal structure of the cyclic peptide **18**. Briefly, we grew apo crystals of the TLE1 WD40 domain using slightly modified previously published conditions<sup>[3]</sup> and succeeded in solving the structure of the cyclic peptide **18** bound to TLE1 to 2.18 Å resolution by soaking with a 2.5 mM solution of **18**. The asymmetric unit contained two TLE1 monomers and electron density was evident in both binding sites. However the quality of the electron density differed in the two independent TLE1 monomers. Chain A showed strong ligand density and allowed us to model the cyclic peptide **18** with full occupancy. The ligand density in chain B was weaker and refined at a lower occupancy (0.83). Therefore we will focus the discussion on the peptide bound to chain A.

Figure 5 depicts the constrained peptide bound to TLE1 and an overlay with the published structure of our acyclic design template, SMWRPW (pdb code 2CE9).

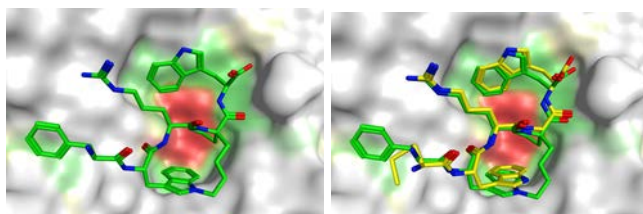


**Figure 5.** Left. Co-crystal structure of the constrained peptide **18** bound to the WDR domain of TLE1. Right. Superposition of the acyclic (yellow) and cyclic (green) peptides **1** and **18**.

Overall, the binding mode of the constrained peptide is almost identical to that of the published acyclic peptide bound structure. The overall root-mean-square deviation (RMSD) between the two structures is 0.55 Å. The N-terminal phenylalanine side-chain of the constrained peptide occupies a similar position as the methionine side-chain with the aromatic side chain efficiently packing against the hydrophobic part of Glu 550, potentially explaining the slightly higher affinity of the acyclic FWRPW compared to the MWRPW peptide. The most significant difference between the cyclic peptide conformation compared to the bound SMRWPW conformation is the linker, which appears to cause a slight change in position of the N-terminal tryptophan and could go some way in explaining the lower affinity of **18** as compared with the linear FWRPW peptide. This slight movement may create an unfavourable, modestly repulsive interaction that outweighs the gain achieved through constraining the peptide. The observation that our cyclic peptide shows a higher  $K_d$  despite replicating the bioactive conformation very accurately underscores the challenge of designing constrained peptides. Minor differences that are outside the predictive power of current structure based design tools, even if high resolution crystal structures are available, can have a significant effect on bioactivity.

## Conclusion

TLE1 is a transcriptional co-repressor that exerts its oncogenic function through binding to transcription factors. Inhibition of this protein-protein interaction represents a putative cancer target but no small molecule inhibitors targeting this challenging interface have been published to date. In this manuscript, we report the design and synthesis of a constrained peptide inhibitor of TLE1.

We developed a concise synthetic route to a constrained proof of concept peptide cycFWRPW (**18**). Biophysical analysis by ITC and thermal shift assays and X-ray crystallography confirmed that the constrained peptide binds to the WD40 domain of TLE1. Furthermore, the observation that the constrained peptide shows binding thermodynamics that are entropically favoured compared to the acyclic FWRPW peptide is in agreement with the hypothesis that rigidifying the peptide lowered the entropic penalty upon binding to the target. However, the constrained peptide also showed an approximately 6-fold lower affinity as compared to the acyclic peptide. The crystal structure of the constrained peptide bound to TLE1 suggests that the linker causes some strain in the molecule that may, at least partially, explain the lower affinity. These observations underscore the known challenge of designing constrained peptides. Our constrained peptide replicated the bioactive conformation very well with an RMSD of 0.55 Å and yet a slight deviation caused a sufficient penalty to compensate the gain achieved by introducing the constraint.

## Experimental Section

### Supporting Information

Experimental and characterization details for all new compounds, computational data, ITC data, assays data, crystallographic data, and NMR spectra are provided free of charge at [link](#).

### Accession codes

Atomic coordinates and structure factors for the crystal structure of TLE1 with constrained peptide **18** can be accessed using PDB code: 5MWJ

## AUTHOR INFORMATION

### Corresponding Author

[swen.hoelder@icr.ac.uk](mailto:swen.hoelder@icr.ac.uk)

### Notes

The authors declare no competing financial interest.

## ACKNOWLEDGMENTS

Lewis Vidler was funded by Cancer Research UK [grant number C309/A11369], Sally McGrath was funded by Wellcome Trust [grant number 090171/Z/09/Z]. We acknowledge NHS funding to the NIHR Biomedical Research Centre and funding from [Cancer Research UK](#) [grant number C309/A11566]. We are grateful to Laurence Pearl, University of Sussex, Brighton, UK for his gift of the construct of the TLE1 WD40 domain. We thank Dr Nora Cronin and the staff of DIAMOND Light Source for their support during data collection.

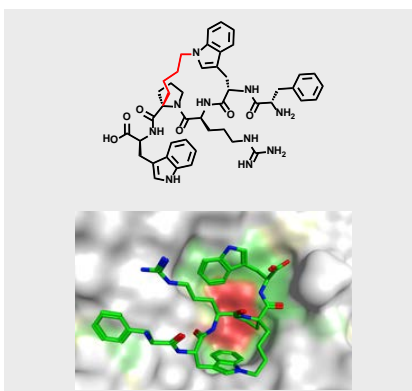
**Keywords:** constrained peptide 1 • protein-protein interaction 2 • inhibitor design 3 • structure based design 4 • cancer 5

- [1] a) B. H. Jennings and D. Ish-Horowicz, *Genome Biol* **2008**, *9*, 205; b) G. Chen and A. J. Courey, *Gene* **2000**, *249*, 1-16.G.  
[2] a) W. C. Foo, M. W. Cruise, M. R. Wick and J. L. Hornick, *Am J Clin Pathol* **2011**, *135*, 839-844; b) K. A. Holmes, A. Hurtado, G. D. Brown, R. Launchbury, C. S. Ross-Innes, J. Hadfield, D. T. Odom and J. S. Carroll, *Proc. Natl. Acad. Sci. U. S. A.* **2012**, *109*, 2748-2753, S2748/2741-S2748/2745; c) T. Knoesel, S. Heretsch, A. Altendorf-Hofmann, P. Richter, K. Katenkamp, D. Katenkamp, A. Berndt and I. Petersen, *Eur. J. Cancer* **2010**, *46*, 1170-1176; d)

- S. W. Seo, H. Lee, H.-I. Lee and H.-S. Kim, *J. Orthop. Res.* **2011**, *29*, 1131-1136; e) X. Yao, S. K. Ireland, T. Pham, B. Temple, R. Chen, M. H. G. Raj and H. Biliran, *Biochem. Biophys. Res. Commun.* **2014**, *455*, 277-284.  
[3] B. H. Jennings, L. M. Pickles, S. M. Wainwright, S. M. Roe, L. H. Pearl and D. Ish-Horowicz, *Molecular Cell* **2006**, *22*, 645-655.  
[4] a) T. A. Hill, N. E. Shepherd, F. Diness and D. P. Fairlie, *Angewandte Chemie International Edition* **2014**, *53*, 13020-13041; b) L. D. Walensky and G. H. Bird, *J. Med. Chem.* **2014**, *57*, 6275-6288; c) P. M. Cromm, J. Spiegel, T. N. Grossmann, P. M. Cromm, J. Spiegel, T. N. Grossmann and T. N. Grossmann, *ACS Chem Biol* **2015**, *10*, 1362-1375; d) C. M. Haney and W. S. Horne, *Org. Biomol. Chem.* **2015**, *13*, 4183-4189.  
[5] Q. Chu, R. E. Moellering, G. J. Hilinski, Y.-W. Kim, T. N. Grossmann, J. T. H. Yeh and G. L. Verdine, *MedChemComm* **2015**, *6*, 111-119.  
[6] S. Yamada, T. Shioiri, T. Itaya, T. Hara, R. Matsueda, *Chemical and Pharmaceutical Bulletin (Tokyo)* **1965**, *13*, 88-93; G. Kumaraswamy, A. Pitchaiah, G. Ramakrishna, D. S. Ramakrishna, K. Sadaiah, *Tet. Lett.* **2006**, *47*, 2013-2015.  
[7] N. Halland, H. Blum, C. Buning, M. Kohlmann and A. Lindenschmidt, *ACS Med. Chem. Lett.* **2014**, *5*, 193-198.  
[8] M. Scholl, S. Ding, C. W. Lee, R. H. Grubbs, *Org. Lett.* **1999**, *1*, 953-956.  
[9] S. H. Hong, M. W. Day, R. H. Grubbs, *J. Am. Chem. Soc.* **2004**, *126*, 7414-7415; S. H. Hong, D. P. Sanders, C. W. Lee, R. H. Grubbs, *J. Am. Chem. Soc.* **2005**, *127*, 17160-17161.  
[10] F. H. Niesen, H. Berglund and M. Vedadi, *Nat. Protocols* **2007**, *2*, 2212-2221.  
[11] G. Klebe, *Nat Rev Drug Discov* **2015**, *14*, 95-110.

## FULL PAPER

Text for Table of Contents



Sally McGrath,<sup>[a]</sup> Marcello Tortorici,<sup>[a]</sup>  
Ludovic Drouin,<sup>[a]</sup> Savade Solanki,<sup>[a]</sup>  
Lewis Vidler,<sup>[a]</sup> Isaac Westwood,<sup>[a]</sup> Peter  
Gimeson,<sup>[b]</sup> Rob Van Montfort,<sup>[a]</sup> Swen  
Hoelder<sup>\*[a]</sup>

**Page No. – Page No.**

**Title**